Drug Resistance Updates 71 (2023) 101007

Contents lists available at ScienceDirect

Drug Resistance Updates

journal homepage: www.elsevier.com/locate/drup

Effective targeting of breast cancer by the inhibition of P-glycoprotein mediated removal of toxic lipid peroxidation byproducts from drug tolerant persister cells

Kornélia Szebényi [a,b,**,1], András Füredi [a,b,c,1], Eszter Bajtai [a,b,d], Sai Nagender Sama [a], Agnes Csiszar [a], Balázs Gombos [b,e], Pál Szabó [f], Michael Grusch [a], Gergely Szakács [a,b,*]

[a] Center for Cancer Research, Medical University of Vienna, Vienna, Austria
[b] Institute of Enzymology, Research Centre for Natural Sciences, Budapest, Hungary
[c] Institute of Technical Physics and Materials Science, Centre of Energy Research, Budapest, Hungary
[d] Doctoral School of Pathological Sciences, Semmelweis University, Budapest, Hungary
[e] Doctoral School of Molecular Medicine, Semmelweis University, Budapest, Hungary
[f] Centre for Structural Study, Research Centre for Natural Sciences, Budapest, Hungary

ARTICLE INFO

Keywords:
Multidrug resistance
P-glycoprotein
Drug-tolerant persister
Tariquidar
Genetically engineered mouse model of cancer
Triple-negative breast cancer

ABSTRACT

Therapy resistance has long been considered to occur through the selection of pre-existing clones equipped to survive and quickly regrow, or through the acquisition of mutations during chemotherapy. Here we show that following in vitro treatment by chemotherapy, epithelial breast cancer cells adopt a transient drug tolerant phenotype characterized by cell cycle arrest, epithelial-to-mesenchymal transition (EMT) and the reversible upregulation of the multidrug resistance (MDR) efflux transporter P-glycoprotein (P-gp). The drug tolerant persister (DTP) state is reversible, as cells eventually resume proliferation, giving rise to a cell population resembling the initial, drug-naïve cell lines. However, recovery after doxorubicin treatment is almost completely eliminated when DTP cells are cultured in the presence of the P-gp inhibitor Tariquidar. Mechanistically, P-gp contributes to the survival of DTP cells by removing reactive oxygen species-induced lipid peroxidation products resulting from doxorubicin exposure. In vivo, prolonged administration of Tariquidar during doxorubicin treatment holidays resulted in a significant increase of the overall survival of *Brca1*$^{-/-}$;*p53*$^{-/-}$ mammary tumor bearing mice. These results indicate that prolonged administration of a P-gp inhibitor during drug holidays would likely benefit patients without the risk of aggravated side effects related to the concomitantly administered toxic chemotherapy. Effective targeting of DTPs through the inhibition of P-glycoprotein may result in a paradigm shift, changing the focus from countering drug resistance mechanisms to preventing or delaying therapy resistance.

Introduction

Therapy resistance remains a major impediment to successful treatment of metastatic cancer. In addition to drug- and target-specific mechanisms, cancer cells can develop simultaneous resistance to multiple, structurally unrelated compounds. Acquired multidrug resistance is associated with the increased expression of drug transporters such as P-glycoprotein (ABCB1/P-gp), which keep cellular levels of chemotherapeutic drugs below a cell-killing threshold. Overexpression of P-gp has been observed in drug-resistant cell lines generated through exposure to increasing concentrations of cytotoxic drugs. P-gp expression is well-characterized in hematological malignancies, sarcomas, breast cancer, and other solid cancers and is frequently correlated with poor clinical response to chemotherapy (Szakács et al., 2006). The role of

Abbreviations: ABC, ATP-binding cassette (ABC); DTP, Drug-tolerant persister; MDR, multidrug resistance; MMP, Matched molecular pair; P-gp, P-glycoprotein (ABCB1); TQ, Tariquidar.

* Correspondence to: Center for Cancer Research, Medical University of Vienna, Borschkegasse 8a, Vienna 1090, Austria.
** Correspondence to: Institute of Enzymology, Research Centre for Natural Sciences, Magyar tudosok korutja 2, Budapest 1117, Hungary.
E-mail addresses: szebenyi.kornelia@ttk.hu (K. Szebényi), gergely.szakacs@meduniwien.ac.at (G. Szakács).
[1] These authors contributed equally to this work.

https://doi.org/10.1016/j.drup.2023.101007
Received 19 May 2023; Received in revised form 11 September 2023; Accepted 13 September 2023
Available online 17 September 2023

cellular drug efflux in acquired resistance to chemotherapy was further demonstrated in a genetically engineered mouse model of hereditary triple-negative breast cancer (TNBC), which closely mimics many aspects of cancer in human patients (Duarte et al., 2018). Like most human cancers, murine *Brca1*$^{-/-}$;*p53*$^{-/-}$ tumors show initial sensitivity, but they invariably acquire resistance to docetaxel, doxorubicin, topotecan, olaparib or Doxil (liposomal doxorubicin) treatments, based on the increased expression of the *Abcb1* or *Abcg2* genes (Füredi et al., 2017a; Rottenberg and Borst, 2012). TNBC is the most lethal subtype of human breast cancer, characterized by early relapse and poor overall survival. In lack of treatment options with targeted and biological agents commonly used in other breast cancer subtypes, cytotoxic chemotherapy remains the only approved treatment of early TNBC, frequently administered in the neoadjuvant setting. Unfortunately, residual disease is detected at surgery in about 80 % of the cases, and this insensitivity to chemotherapy is associated with a higher risk of recurrence, distant metastasis and death compared to non-TNBC (Liedtke et al., 2008). Protocols resulting in the highest possible remission rates are still being determined. In the adjuvant setting, third generation chemotherapy regimens utilizing dose-dense or metronomic polychemotherapy are among the most effective tools presently available (Isakoff, 2010). Unfortunately, resistance to these therapies emerges quickly, and therefore effective treatment of TNBC represents an unmet clinical need (Harbeck et al., 2019). While P-gp is commonly overexpressed in TNBC (Zhao et al., 2020), mechanisms underlying therapy resistance of triple-negative breast cancer are not known. It is yet unclear whether chemoresistance in TNBC is linked to genomic and/or nongenomic mechanisms. Resistance often occurs through the selection of small pre-existing subpopulations or through the acquisition of mutations during chemotherapy (Russo et al., 2019). Alternatively, relapse may depend on a critical subpopulation of drug tolerant persister (DTP) cells, which undergo reversible phenotypic transitions to replenish the tumor over and over again, until mechanisms ensuring stable drug resistance emerge (Borst, 2012). DTP cells underlie minimal residual disease (MRD), providing a reservoir for chemo-sensitive relapse and the eventual emergence of heterogeneous drug-resistance mechanisms (Ramirez et al., 2016). Studies performed on patient derived xenografts indicated that resistance is mediated by nonselective mechanisms that confer a reversible chemotherapy-tolerant state. Barcode-mediated clonal tracking and genomic sequencing of PDX tumors established from TNBC patients revealed that residual tumors consisting of DTP cells give rise to sensitive tumors with similar transcriptomes, proteomes, and histological features to those of untreated tumors (Echeverria et al., 2019).

Recent studies have clarified the molecular underpinning of DTP hallmarks that include slow proliferation, phenotypic plasticity, environmental adaptation and altered metabolism (reviewed in (Shen et al., 2020)). In addition to epigenetic reprograming (Liau et al., 2017; Sharma et al., 2010), dormancy or slow proliferation is attributed to the concerted downregulation of the Myc, mTOR and various cell-cycle related pathways as well as the shutdown of protein synthesis, akin to the transient pause of embryonic development triggered by unfavorable environmental conditions (Rehman et al., 2021). DTP cells adopt a range of phenotypes through EMT-related transitions and trans-differentiation (Shen et al., 2020; Risom et al., 2018). Consistent with their slow proliferation, DTP cells rely on mitochondrial respiration, autophagy and peroxisomal fatty acid β-oxidation (Roesch et al., 2013). Because of the increased mitochondrial respiration, DTPs are highly dependent on anti-oxidative protection provided by the glutathione peroxidase GPX4 and more generally the thioredox detoxifying pathway, controlled by the master regulator of redox homeostasis NRF2 (Aissa et al., 2021; Hangauer et al., 2017; Viswanathan et al., 2017). In summary, DTPs adopt evolutionary conserved programs orchestrating cellular stress responses that favor cell survival in extreme conditions. In this work our aim was to assess the relevance of P-gp, which is one of the best characterized effectors of the evolutionary conserved cellular detoxification pathway. We show that the transient upregulation of the drug efflux pump P-gp induced by doxorubicin is needed for the survival of DTP cells, revealing a vulnerability that can be exploited by a clinically available transporter inhibitor.

Materials and methods

Drugs

Cytotoxic drugs doxorubicin (TEVA), Olaparib (Selleckchem) and cisplatin (Accord Healthcare) were purchased directly from the manufacturers. Tariquidar was a kind gift from Susan E. Bates (National Cancer Institute).

Cell lines

The human breast cancer cell lines MCF7 (estrogen receptor (ER) positive cell line derived from the pleural effusion of a breast adenocarcinoma), T47D (invasive breast carcinoma of no special type), and MDAMB468 (TNBC), were obtained from the National Cancer Institute's Developmental Therapeutics Program (National Institutes of Health). The A431 cell line was obtained from ATCC. ABCB1 was expressed in A431 and MCF7 cells by lentiviral transduction (Cserepes et al., 2020; Pape et al., 2015). Functional expression of ABCB1 was confirmed by flow cytometry analysis (Supplementary Figure 12). Extra attention was paid to preserve sterility of the long-term repopulation assays. The cell lines were cultured in RPMI media (Life Technologies) supplemented with 10 % fetal bovine serum, 5 mmol/L glutamine, and 100 units/mL penicillin and streptomycin (Life Technologies), using disposable serological pipettes. All cell lines were cultured at 37 °C, 5 % CO2.

In vitro cytotoxicity assay

Viability was assessed by the PrestoBlue® assay (Life Technologies, USA), according to the manufacturer's instructions. Briefly, cells were plated in 96-well plates, treated in the given concentration range with the indicated compounds for 120 h to determine IC_{30} values for treatment. Viability of the cells was measured spectrophotometrically using an Infinite M200 microplate reader (Tecan Life Sciences). Curves were fitted by Graph Pad Prism 5 software using the sigmoidal dose–response model. Curve fit statistics were used to determine IC_{50} and IC_{30} values. Differences between the IC values were analyzed by two-sided unpaired Student's t test and results were considered statistically significant at a P value of <0.05 (*) or 0.01 (**).

UO126 treatment

Cells (8×10^5 in the case of MCF7, 10^6 in the case of MDAMB468 and T47D) were plated in T25 flasks and were kept in RPMI media (Life Technologies) supplemented with 10 % fetal bovine serum, 5 mmol/L glutamine, and 100 units/mL penicillin and streptomycin (Life Technologies) for 24 h before 15 μM UO126 was added to the cultures. An hour after adding UO126, half of the flasks received an additional doxorubicin treatment (MCF7: 220 nM, T47D: 120 nM, MDAMB468: 50 nM). Those cultures which were pretreated with UO126 on day 1, received a second treatment of 15 μM UO126 on day 3. On day 4 cultures treated with doxorubicin only, or in combination with UO126 were collected and 10^5 cells per condition were stained against ABCB1 (MRK16, Kamiya Biomedical, 1:200) or mouse IgG2a isotype control (Santa Cruz Biotechnology, sc-3878) with Goat anti-Mouse IgG2a-PE secondary antibody (ThermoFisher Scientific, P-21139) for flow cytometry.

Establishment of the G1-mCherry expressing MCF7 cell line

Viral particles were generated in HEK293 cells by co-transfection of

pRetroX-G1-mCherry-puro (encoding the G1-phase cell cycle indicator mCherryhCdt1) purchased from Takara (cat#631463), with the helper plasmids pVSV-G (Clontech) and p-gag-pol-gpt (Markowitz et al., 1988). Supernatants were used to transduce MCF7 cells grown to 50 % confluency in 6-well plates. Cells were selected with 0.8 μg/mL puromycin for 10 days, and transgene expression was monitored under an epifluorescent microscope (Nikon Eclipse).

Live-cell microscopy

5×10^4 MCF7-G1-Red cells/well were seeded in 24 well plates 24 h before treatment. 220 nM doxorubicin (DOX), 130 μM cisplatin (CIS) or 200 uM Olaparib (OLA) were added to the cells for 120 h and live-cell fluorescent imaging was performed using a JuLI Stage automated microscope (NanoEntek) inside a standard cell incubator. Images were taken every 30 min.

CytoTell cell proliferation assay

CytoTell Green (AAT Bioquest) working solution was added to non-treated or DOX-treated MCF7 cells on day 12 (D5 + 1). After incubating the cells on 37 °C for 30 min, CytoTell was replaced with culture media. On D5 + 1 and D5 + 9 cells were collected for flow cytometry analysis. Fluorescence signal was measured using an Attune NXT flow cytometer, dead cells were excluded from analysis based on Zombie Violet Viability Dye (Biolegend).

Immunocytochemistry

Cells (3×10^4 in the case of MCF7 and MDAMB468 or 4×10^4 in the case of T47D) were plated in 8-well chambers (Eppendorf), 24 h later treatment was applied and after 24 h (for H2AX staining), five (for H2AX or ECAD staining), seven (for ABCB1 staining) days or at repopulation (for ECAD and H2AX staining) cells were fixed with 4 % paraformaldehyde for 15 min at room temperature. Control/untreated cells were left to grow for 6 days before fixation. For membrane staining cells were incubated with WGA-Alexa Fluor 488 (Invitrogen) for 30 min at 37 °C before fixation. Following fixation two washing steps were applied with Dulbecco's modified phosphate-buffered saline (DPBS) and cells were treated with blocking solution (DPBS containing 2 mg/mL BSA, 5 % goat serum and 0.1 % Triton-X 100) for 1 h at 4 °C. The samples were then incubated for 3 h at 4 °C with anti-ABCB1 antibody (MRK16, Kamiya Biomedical, 1:200) or anti-E-cadherin antibody (DECMA-1, Abcam, 1:100) or anti-Vimentin antibody (E-5, Santa Cruz Biotechnology, 1:100) in blocking solution. For DNA damage staining anti-Phospho-Histone H2A.X (3F2, ThermoFisher Scientific, 1:500) was used in blocking solution for 1 h at 37 °C. Specifically for staining with the anti-ABCG2 antibody (5D3, BD Pharmingen, 1:200) cells were pre-treated with 5 μM Ko143 for 5 min at 37 °C and Triton-X 100 was omitted from the blocking solution. After washing with DPBS, the cells were incubated for 1 h at 4 °C with Alexa Fluor 488-conjugated goat anti-mouse IgG antibody (Invitrogen) in case of ABCG2, Vimentin and H2AX; with Alexa Fluor 488-conjugated goat anti-mouse IgG2a antibody in case of ABCB1, and with Alexa Fluor 546 conjugated goat anti-rat IgG antibody in case of E-cadherin. Secondary antibodies were diluted in blocking solution (1:250). Nuclei were stained with DAPI (Invitrogen). The stained samples were examined by a Zeiss LSM 700 confocal laser scanning microscope.

Western blotting

Cells were lysed in RIPA buffer (150 mM NaCl, 50 mM Tris pH 7.4, 1 % Nonidet P40, 1 % Na-deoxycholate, 1 mM EDTA, 1 mM Na_3VO_4, 25 mM NaF) supplemented with Complete protease inhibitor cocktail (Roche). Equal amounts of lysates were analyzed by SDA-PAGE after total protein quantification by Bradford protein assay (Bio-Rad). Proteins were transferred onto PVDF membranes (Immobilon®-P); the identity of the bands were revealed by phosphoErk1/2, Erk1/2 and Hsp90 primary antibodies (Cell Signaling Technology) and HRP-coupled secondary antibodies (Jackson ImmunoResearch). Blots were developed using Clarity ECL Substrate and Chemidoc Touch device (Bio-Rad) and analyzed in ImageLab software (Bio-Rad).

RNA isolation and RT-PCR

Cells were collected in TRIzol™ Reagent (Life Technologies). Total RNA was isolated using Direct-zol® MiniPrep kit (Zymo Research) according to the manufacturer's guidelines. In-column DNAse I treatment was applied to prevent DNA contamination. cDNA samples were prepared from 1 μg total RNA using the Promega Reverse Transcription System Kit. The Pre-Developed TaqMan® assay Ribosomal Protein Lateral Stalk Subunit P0 (RPLP0, Life Technologies) was used as endogenous control in real-time qPCR experiments; mRNA levels were quantified by TaqMan® primers. Real-time PCR analyses were carried out using the StepOne™ Real-Time PCR System (Life Technologies); mRNA fold changes were determined using the $2^{-\Delta\Delta Ct}$ method. Relative mRNA levels are presented as mean values ± SD of 3 independent experiments.

In vivo experiments

All animal protocols were approved by the Hungarian Animal Health and Animal Welfare Directorate according to the EU's most recent directives. All surgical procedures were performed according to the Committee on the Care and Use of Laboratory Animals of the Council on Animal Care at the Institute of Enzymology, Research Centre for Natural Sciences in Budapest, Hungary (22.1/2291/3/2010).

Tissue pieces (1–2 mm in diameter) obtained from *Brca1*$^{-/-}$*;p53*$^{-/-}$ and *Brca1*$^{-/-}$*;p53*$^{-/-}$*;Abcb1a/b*$^{-/-}$ FVB mouse mammary tumors (a kind gift from Sven Rottenberg, NKI) were transplanted orthotopically into the mammary fat pad of wild type female FVB mice (Harlan) under anesthesia (20 mg/kg zolazepam, 12.5 mg/kg xylazine, 3 mg/kg butorphanol, 20 mg/kg tiletamine) (Hámori et al., 2020). The tumor size was monitored at least 3 times per week by caliper measurements after the tumors became palpable. Tumor volume was calculated using the $V = (\text{length} \times \text{width}^2)/2$ formula. When the volume of the tumors reached ~200 mm^3, DOX treatment was initiated using the maximum tolerable dose (MTD, 5 mg/kg iv respectively) alone or in various combinations with ABCB1 inhibitor Tariquidar (15 mg/kg iv). Treatments using the MTD were repeated every 10 days unless the size of the tumors decreased to 50 % of its original volume. In that case treatment was repeated when the tumor relapsed to its original size. Animals were sacrificed when the tumor volume reached ~3000 mm^3.

Calcein AM assay

Calcein AM assay was performed to assess P-gp function in cells isolated from mouse mammary tumors as described before (Füredi et al., 2017b). Briefly, pieces from a freshly removed tumor were transferred to a 50-mL conical tube containing 20 mL of 200 U/mL type IV collagenase and 0.6 U/mL dispase (Life Technologies) in completed DMEM and digested for 2 h at 37 °C with vortexing every 15 min for 1 min. The cell suspension was filtered through a 70-mm nylon filter insert (BD Biosciences) and centrifuged for 5 min at 300g. The supernatant was removed, the pellet was dissolved in completed DMEM/F-12 and viable cell number was determined using a TC-10 cell counter (Bio-Rad). 250,000 isolated primary tumor or A431 cells were incubated with 0.25 mmol/L calcein AM (Dojindo Molecular Technologies) with or without 10 μmol/L verapamil for 10 min at 37 °C. Cells were washed with ice-cold PBS, and calcein accumulation was measured with a FACSCANTO II flow cytometer. Dead cells were excluded based on TO-PRO3 (Life Technologies) positivity.

Lipid peroxidation imaging

Lipid peroxidation in A431 and A431-ABCB1 cells was detected using the Click-iT Lipid Peroxidation Imaging kit (Thermo Fisher Scientific) according to the manufacturer's guidelines. Briefly, 10^5 cells were plated on 24-well plates and incubated overnight at 37 °C and 5 % CO_2. Linoleamide alkyne (LAA) reagent was added to the cultures in complete growth medium and immediately followed by 10 mM AAPH (2,2′-Azobis(2-methylpropionamidine) dihydrochloride) treatment with or without 1 μM Tariquidar. After a 24-hour treatment cells were washed twice with PBS, fixed with 4 % PFA for 15 min, permeabilized with 0.5 % Triton® X-100 for 10 min and blocked by 1 % BSA-PBS for 30 min at room temperature. Cells were then incubated with Click-iT reaction cocktail containing Alexa Fluor 488 for 30 min to detect lipid peroxidation product of LAA, washed with PBS and imaged with JuLI Stage automated microscope.

Malondialdehyde (MDA) assay

The assay was performed according to the manufacturer's guidelines. Briefly, A431, A431-B1, MCF7 and MCF7-B1 cells were treated with 10 mM AAPH for 48 h and 10^6 cells were homogenized in MDA Lysis Buffer with BHT. Samples were centrifuged for 10 min at 13.000g and the supernatant were transferred into a microcentrifuge tube. Samples were treated with TBA, incubated for 1 h at 95 °C then fluorescence was measured using 532 nm excitation and 553 nm emission using an Enspire multimode plate reader (Perkin Elmer).

Glutathione peroxidase assay

Glutathione peroxidase activity was measured using the Glutathione Peroxidase Assay Kit (Sigma) according to the manufacturer's protocol. Briefly, untreated and DOX or DOX+TQ treated cells were harvested at Day 5, homogenized in ice-cold PBS with a Dounce tissue grinder, centrifuged at 14.000 g for 10 min, and the clear supernatant was snap-frozen and stored at –80 °C until further use. 10 μl of the thawed supernatant was mixed with 90 μl Working Reagent and 100 μl Substrate Solution and immediately measured at 340 nm in absorbance mode with a EnSpire (Perkin Elmer) multimode plater reader. All experiments were performed at least 3 times.

ROS determination using DCFDA

Generation of reactive oxygen species was quantified by the

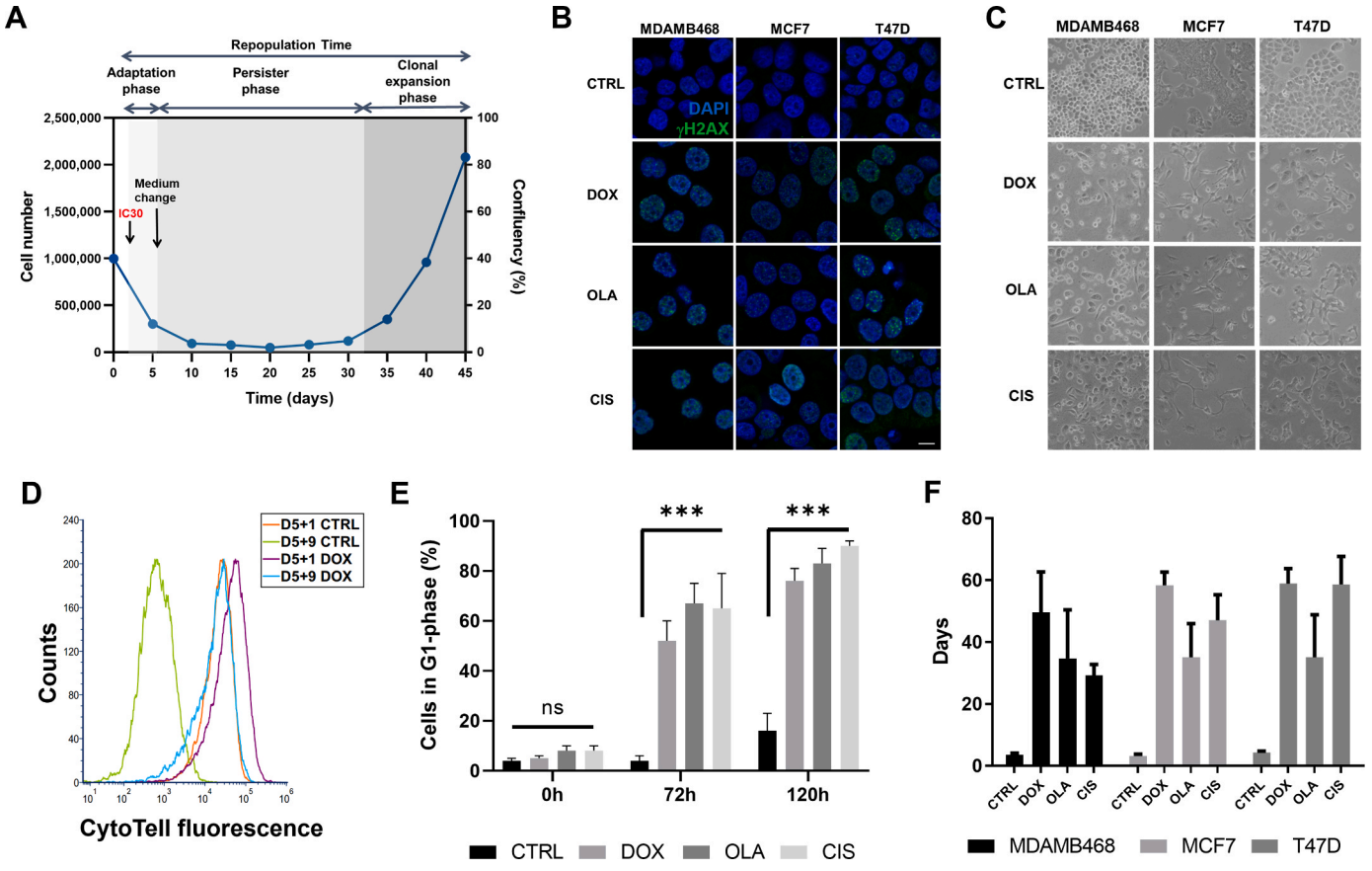

Fig. 1. Repopulation of breast cancer cell cultures from a reservoir of DTP cells following in vitro treatment with doxorubicin (DOX), cisplatin (CIS) or Olaparib (OLA) (A) Schematic representation of the established in vitro assay designed to study the drug-tolerant persister state. T47D cells were treated with IC_{30} DOX for 5 days; surviving cells were followed in drug-free medium. Cell numbers were determined using a TC-10 automated cell counter. (B) Immunofluorescence detection of DNA damage of breast cancer cells treated for 5 days with the IC_{30} concentrations of the indicated drugs. Nuclei were stained with DAPI (blue); double stranded breaks were detected by a phospho-H2AX antibody (green). Scale bar: 10 μm. (C) Phase contrast images showing morphological changes during the adaptation phase (5 days after drug treatment). (D) Cell divisions monitored by the CytoTell fluorescent label-dilution assay over 8 days. MCF7 cells were treated with DOX for 5 days; baseline fluorescence of the persister cells was recorded by flow cytometry one day after the removal of the drug (D5 + 1 DOX, purple). Baseline fluorescence of untreated cells was recorded at similar confluency (D5 + 1 CTRL, red). Fluorescence of DOX-treated (D5 + 9 DOX, blue) and control (D5 + 9 CTRL, green) cells was recorded 8 days later. (E) Image-based cell cycle profiling of MCF7 cells expressing the G1-phase indicator mCherry-hCdt1 after treatment with IC_{30} concentrations of the indicated drugs for 5 days. The proportion of cells in G1 phase was determined by video microscopy (see Supplementary Fig. 2 and Supplementary Video 1 for more details). (F) Repopulation time of breast cancer cells after treatment with IC_{30} concentrations of DOX, OLA or CIS.

Dichlorodihydrofluorescein diacetate (DCFDA) assay, using the Cellular ROS Assay Kit (Abcam). Briefly, 10^6 cells were treated with either DOX or DOX+TQ for 5 days and further cultured for 2 additional days in drug-free medium. Both 5- and 7-day samples were investigated by staining cells with 20 μM DCFDA for 4 h in a 37 °C water bath (Pape et al., 2021). Samples were analyzed by an Attune flow cytometer. As a positive control, cells were treated with 50 μM tert-butyl hydrogen peroxide (t-BHP) for 3.5 h after DCFDA staining. Untreated cells served as negative controls.

Results

Establishment of an in vitro assay to study drug-induced persister cells

To model acute drug response and to generate DTP cells, we established an in vitro assay using three human epithelial breast cancer cell lines. MCF7, T47D and MDAMB468 cells were treated with doxorubicin (DOX), cisplatin (CIS) or Olaparib (OLA). To simulate high-dose chemotherapy, the protocol consisted of a single, high-dose (IC_{30}) treatment lasting for 5 days, which killed the majority of cells (Fig. 1A, Supplementary Fig. 1A,B). Following the addition of drugs, three phases were distinguished based on microscopic imaging. Within the first 2 days of treatment, cells showed significant DNA damage, which was accompanied by massive cell death, a loss of epithelial cobblestone-morphology, and the appearance of individual spindle-shaped cells (adaptation phase, Fig. 1B,C). Following drug removal, the medium was replaced weekly to monitor surviving cells in the persister phase. Live cell video microscopy revealed that cells progressively accumulated in G1 phase, resulting in complete growth arrest (Fig. 1 D,E Supplementary Fig. 2, Supplementary video 1). DTP cells remained quiescent for several weeks, until some of the dormant cells suddenly reentered the cell cycle to give rise to new cell clones ("clonal expansion"). Because of the extremely long persister phase, repopulation of the flasks from the DTP cells occurred in 1–2 months (Fig. 1F).

Short-term, high-dose drug exposure leads to EMT-like changes and the expression of P-glycoprotein in a subpopulation of human breast cancer cells

Since changes occurring during the adaptation phase may contribute to long-term survival, we further characterized the emerging phenotypes. In all treatment groups, surviving cells exhibited significant morphological changes reminiscent of epithelial-mesenchymal transition (EMT). Disintegration of the tight epithelial colonies was accompanied by the internalization of E-cadherin (Fig. 2A) and a differential expression of EMT transcription factors (Fig. 2B, Supplementary Fig. 3). Treatment with DOX resulted in the upregulation of EMT transcription factors including SNAIL1, SNAIL2, TWIST and ZEB, as well as the increased mRNA expression of Vimentin and N-cadherin (CDH2). Similarly, treatment with OLA and CIS resulted in the upregulation of EMT transcription factors, but the extent and pattern of the changes was cell-line dependent. Long-term selection of cells in chemotherapeutics that are effluxed by MDR pumps almost invariably leads to the overexpression of ABCB1/P-gp or ABCG2 (Szakács et al., 2006). To characterize the expression of the transporters, persister cells were analyzed by immunostainings (Fig. 2C, Supplementary Fig. 4). While the expression of ABCB1 was undetectable in treatment-naïve cells, treatment with DOX or OLA resulted in the upregulation of P-gp in a small subpopulation of persister cells. In contrast, CIS, which is not recognized by the transporter, failed to induce the expression of P-gp (Fig. 2C). Addition of

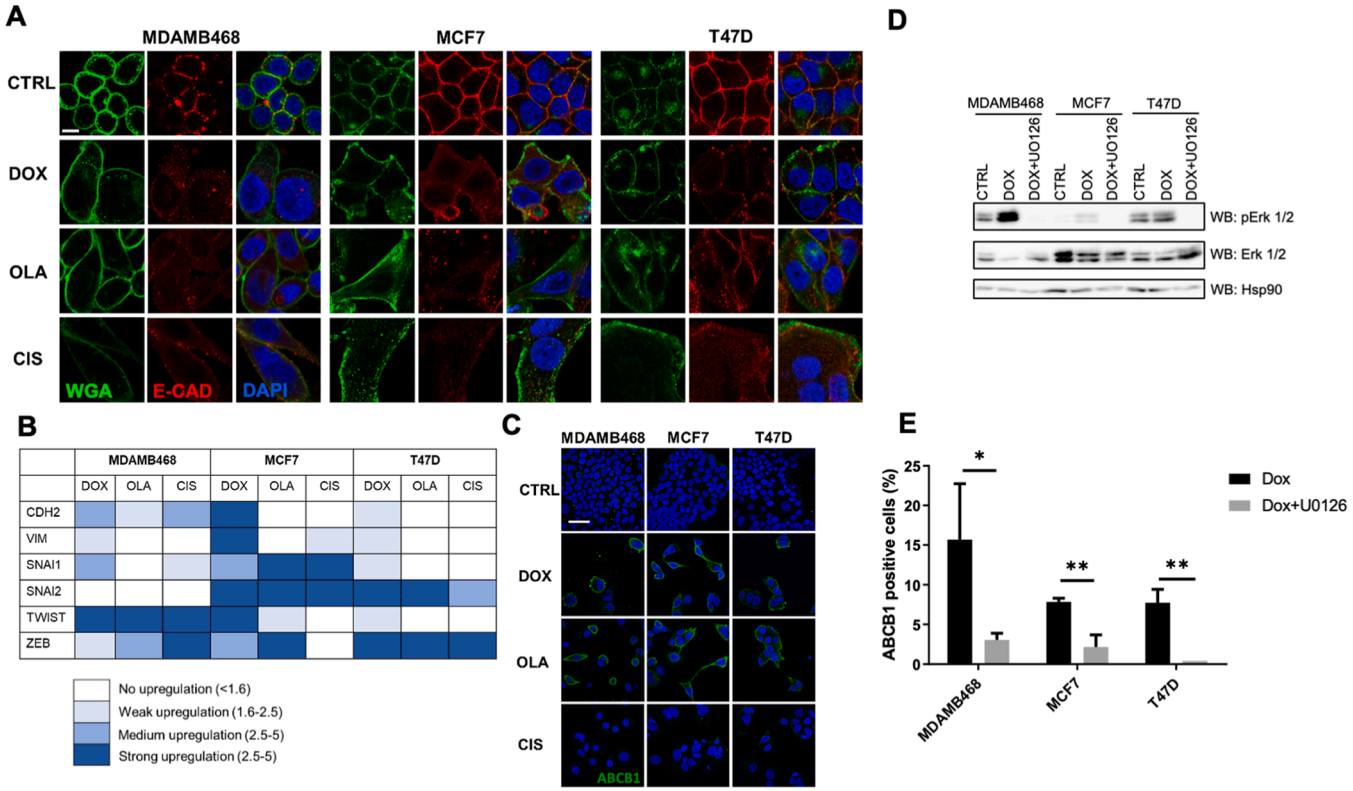

Fig. 2. Chemotherapy induces EMT and ERK-dependent upregulation of P-gp. (A) Immunofluorescent staining of breast cancer cells showing the internalization of E-cadherin (red) from the cell membrane (green) during the adaptation phase. Images were taken after 5 days of treatment with the indicated drugs; nuclei were stained with DAPI (blue). Scale bar: 10 μm. (B) Heat map showing the fold change of master EMT regulator genes 5 days after drug treatment. (C) Immunofluorescence images showing ABCB1/P-gp expression (green) 7 days after treatment with the indicated drugs. Nuclei were stained with DAPI (blue). Scale bar: 50 μm. (D) Western blot analysis of ERK1/2 activity in all cell lines after 4 days of DOX treatment in the presence or absence of the MEK inhibitor UO126. Hsp90 was used as loading control (E) Percentage of P-gp positive cells revealed by flow cytometry after 4 days of DOX treatment in the presence or absence of UO126.

the MAPK/ERK inhibitor U0126 significantly decreased the ratio of P-gp positive cells, confirming the link of Mitogen-Activated Protein Kinase pathways in the doxorubicin-induced upregulation of P-gp (Shukla et al., 2010) (Fig. 2D,E and Supplementary Fig. 5), while OLA did not induce the activation of the ERK pathway (Supplementary Fig. 6).

Awakening of drug tolerant persister cells gives rise to cells resembling the drug-naïve phenotype

Following several weeks of persistence, flasks became rapidly repopulated with the re-awakening of dormant cells. In contrast to the extensive phenotypic changes observed in the adaptation and persister phase, reemerging cells showed the initial epithelial phenotype observed prior to the treatment (Fig. 3A). Significantly, the surge of P-gp expression observed in a subset of DTP cells also proved to be transient and reversible, as P-gp expression could no longer be detected in the repopulated cells (Fig. 3B). Accordingly, repopulating cells were just as sensitive to the applied chemotherapeutics as their treatment-naïve counterparts, proving that the survival of the populations was not mediated by the selection of preexisting resistant cells (Fig. 3C). Following the uniform H2AX-positivity of drug treated cells, the repopulating clones did not exhibit any sign of DNA damage (Fig. 3D). Taken together, results obtained in the in vitro repopulation assay suggested that relapse after the toxic treatment is dependent on the survival of DTP cells that acquire transient phenotypes, and the awakening of dormant cells requires the efficient repair of the DNA.

Transient expression of P-gp promotes the survival of DTPs in DOX-treated cells

Since P-glycoprotein was no longer detected in repopulating cells, we wanted to evaluate the relevance of the transient surge of P-gp expression in the long-term survival of DTP cells. We therefore repeated the in vitro repopulation assay in various combinations involving the specific P-gp inhibitor Tariquidar (TQ), which is devoid of any effect on untreated cells. The long-term effect of TQ on drug-treated cells was analyzed based on the repopulation times of replicate assays (Fig. 4A). Consistent with the lack of P-gp expression in treatment-naïve cells, addition of TQ to the 5-day treatment protocols (DT) did not change the average length of the persister phase, and did not influence survival in short-term cytotoxicity assays (Supplementary Fig. 7). However, when TQ was maintained after the removal of DOX (DT-T-T), repopulation was significantly hindered. Surprisingly, when TQ was only added after the removal of DOX (D-T-T), repopulation was eliminated in 3 of the 4 replicates (Fig. 4A). In the case of Olaparib and cisplatin, no significant differences were found among the conditions. Together, these data show that in the context of DOX treatment, the function of transiently expressed P-gp is critical for the survival and/or the awakening of DTP cells. Although TQ proved effective even after DOX had been removed, it seemed plausible that inhibition of P-gp could influence the accumulation of residual DOX that remained associated with the cells. Indeed, flow cytometry analyses confirmed that all cells treated with doxorubicin exhibited higher fluorescence emitted by the drug, which was maintained in the surviving cells even after the removal of the drug. However, addition of TQ during or after DOX treatment did not change P-gp expression (Supplementary Fig. 8) or DOX fluorescence of the cells

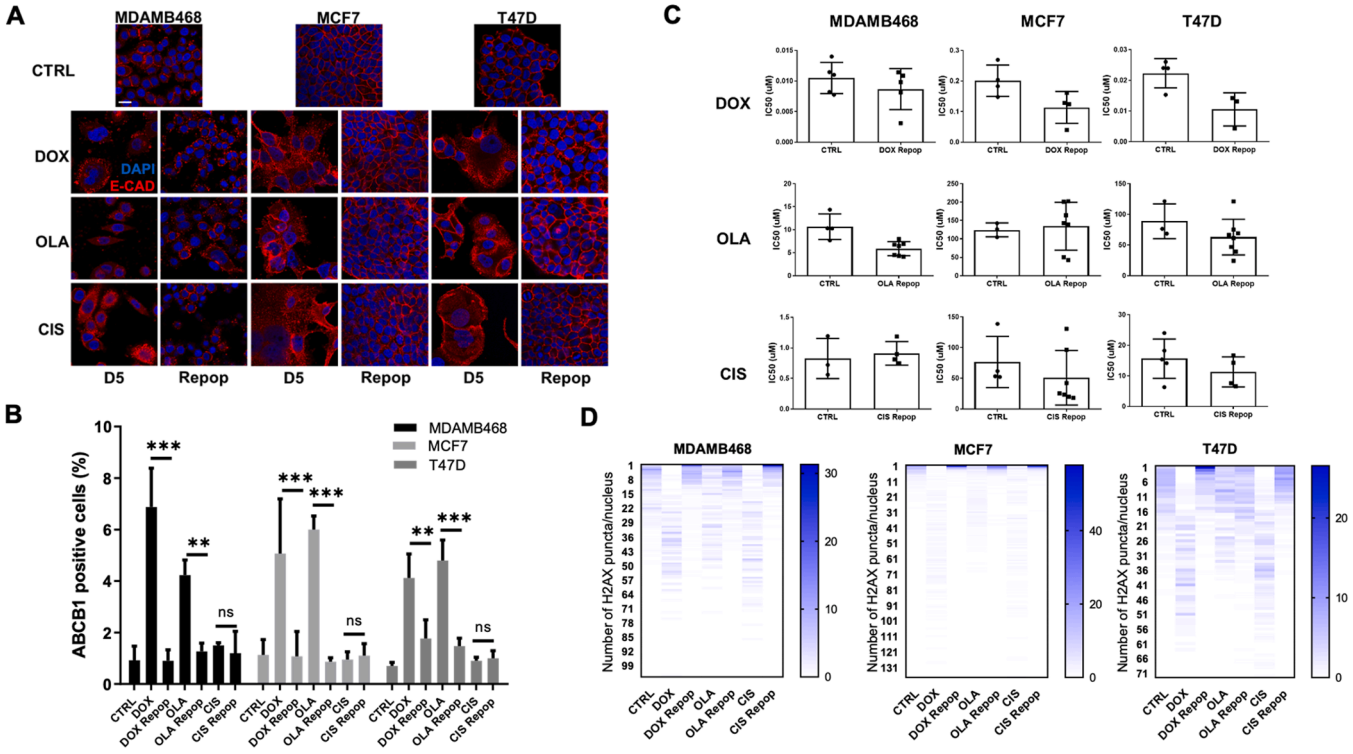

Fig. 3. Drug-tolerant persister cells exhibit transient phenotypes (A) Immunofluorescent staining of breast cancer cells showing localization of E-cadherin (red) in drug-naïve (top), DTP (at day 5, D5) and repopulated cells (Repop). E-cadherin internalization and the EMT-like morphology observed in DTPs is fully reversed in repopulated cells. Scale bar: 20 μm. (B) Percentage of P-gp positive cells in drug naïve, DTP and repopulated breast cancer cell cultures. DOX/OLA-induced expression of P-gp in a subset (4–8 %) of DTP cells is completely reversed in the relapsing cell population. (C) Average IC_{50} values showing the in vitro sensitivity of treatment-naïve, CTRL) and repopulated ("Repop") cells to the applied treatments. (D) Heat map showing the number of H2AX-positive foci per nucleus in drug naïve (CTRL 24 h), DTP (DOX/OLA/CIS 24 h) and repopulated (DOX/OLA/CIS Repop) breast cancer cell cultures. Cells show extensive DNA damage 24 h after drug treatment, whereas repopulating cells are indistinguishable from samples before treatment. DNA damage was quantified by CellProfiler, counting H2AX-positive foci in confocal microscopy images. The color gradient represents the number of cells detected.

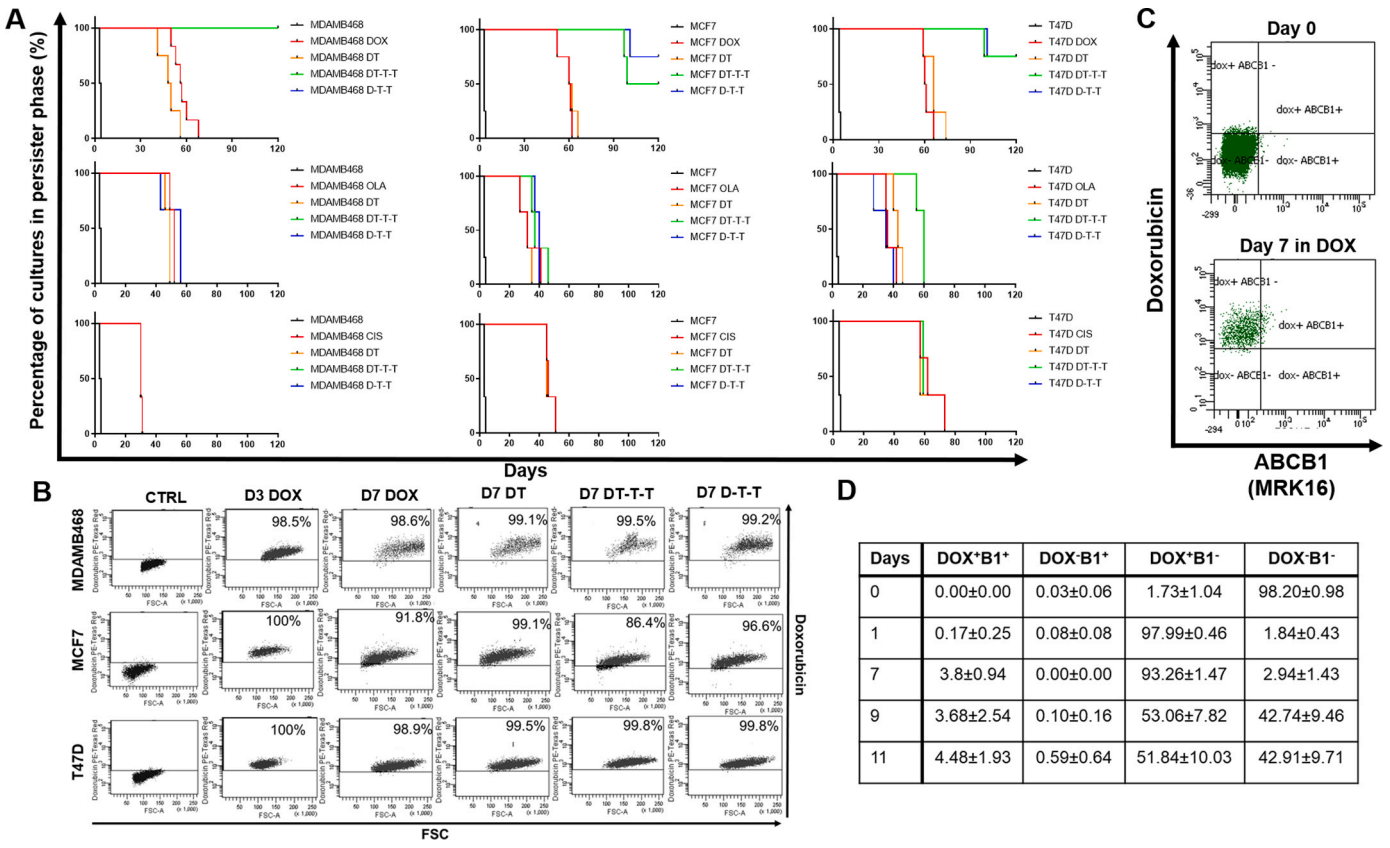

D

Days	DOX⁺B1⁺	DOX⁻B1⁺	DOX⁺B1⁻	DOX⁻B1⁻
0	0.00±0.00	0.03±0.06	1.73±1.04	98.20±0.98
1	0.17±0.25	0.08±0.08	97.99±0.46	1.84±0.43
7	3.8±0.94	0.00±0.00	93.26±1.47	2.94±1.43
9	3.68±2.54	0.10±0.16	53.06±7.82	42.74±9.46
11	4.48±1.93	0.59±0.64	51.84±10.03	42.91±9.71

Fig. 4. Transient induction of P-gp by DOX is crucial for the long-term survival of drug-treated cells. (A) Curves showing the time required for cultures to repopulate after different combination treatment protocols. DOX/OLA/CIS: drug treatment for 5 days, followed by the exchange of medium; DT: Tariquidar (TQ) added with the applied drug for 5 days; DT-T-T: TQ added with the applied drug for 5 days, followed by two additional 3-day-long TQ treatments; D-T-T: drug treatment for 5 days, followed by two additional 3-day-long TQ treatments. (B) Percentage of DOX-positive cells determined by flow cytometry in cells before treatment (CTRL), during DOX treatment (day 3), and 2 days after removing DOX (day 7). (C) Simultaneous analysis of DOX content and ABCB1/P-gp expression levels by FACS before (Day 0) and after 7 days of treatment with DOX. P-gp positive cells appearing at day 7 are confined to the upper right quadrant, indicating that they do not have reduced DOX levels. (D) Quadrant statistics based on DOX content and P-gp expression of triplicate samples, as determined by FACS. Baseline levels represent treatment-naïve cells (day 0). Following treatment with DOX for 7 days (Day 1–7), the medium was exchanged and cells were further monitored without the drug (day 9 and 11). P-gp expressing cells appearing at day 7 remain DOX-positive.

(Fig. 4B), and the subpopulation of DOX-treated cells expressing P-gp did not show reduced DOX fluorescence (Fig. 4C,D). Together, these results indicate that the residual DOX in DTP cells is not amenable to P-gp mediated efflux.

Removal of toxic lipid peroxidation products by P-gp contributes to the survival of DTPs

The role of free radicals and lipid peroxidation in the cytotoxicity of DOX is well documented (Myers et al., 1977; Nabil Benchekroun and Robert, 1992). Indeed, DOX-treatment induced the formation of reactive oxygen species (ROS), which was however not influenced by TQ, indicating that the drug-induced P-gp expression does not attenuate doxorubicin's primary toxicity (Fig. 5A, Supplementary Fig. 9), while OLA failed to induce ROS accumulation (Supplementary Fig. 10). Hangauer and colleagues have shown that the survival of DTPs is dependent on the lipid hydroperoxidase GPX4, which plays a crucial role in the neutralization of toxic lipid peroxidation (LP) byproducts resulting from toxic chemotherapy (Hangauer et al., 2017). In agreement with these results, DOX-tolerant persister cells showed significantly increased GPX activity, which was not influenced by the addition of TQ (Fig. 5B). Given the protective role of P-gp in DTPs revealed by our experiments, we wanted to test whether P-gp can mitigate the lethal effect of ROS-induced LP and thus contribute to the long-term survival and eventual relapse of cancer cells. As expected, treatment with 10 mM of the LP-inducing compound AAPH resulted in an increase in the cellular concentration of malondialdehyde (MDA), a toxic byproduct of lipid peroxidation. Interestingly, increase of AAPH-induced MDA levels was significantly mitigated by P-gp in MCF7-B1 (Supplementary Fig. 11) and A431-B1 cells (Fig. 5C) overexpressing the transporter. Additionally, a 48-hour treatment with 10 mM AAPH completely eliminated parental cells, whereas the P-gp expressing derivative was able to recover after the removal of AAPH, eventually repopulating the flask following a brief persister phase. Co-treatment with TQ prevented the survival of persisters and the repopulation of the culture (Fig. 5D). As expression of P-gp (Supplementary Fig. 12) or the presence of TQ (Supplementary Fig. 13) did not influence the sensitivity of MCF7 and A431 cells towards the LP-inducing compound AAPH, it could be excluded that these results were a consequence of the efflux of AAPH by P-gp. Quantification of lipid peroxidation byproducts (Fig. 5E) indicated that unless treated by TQ, P-gp overexpressing cells survive AAPH treatment by removing lipid peroxidation-derived toxic byproducts (Supplementary Fig. 14).

Prolonged administration of Tariquidar in drug-sensitive Brca1$^{-/-}$;p53$^{-/-}$ mouse mammary tumors increases response to doxorubicin treatment

Our results obtained in the in vitro repopulation assay suggested that inhibition of P-gp in DTP cells can influence the outcome of DOX treatment prior to the development of resistance. To test the strategy of prolonged P-gp inhibition during the persister phase, *Brca1$^{-/-}$;p53$^{-/-}$*

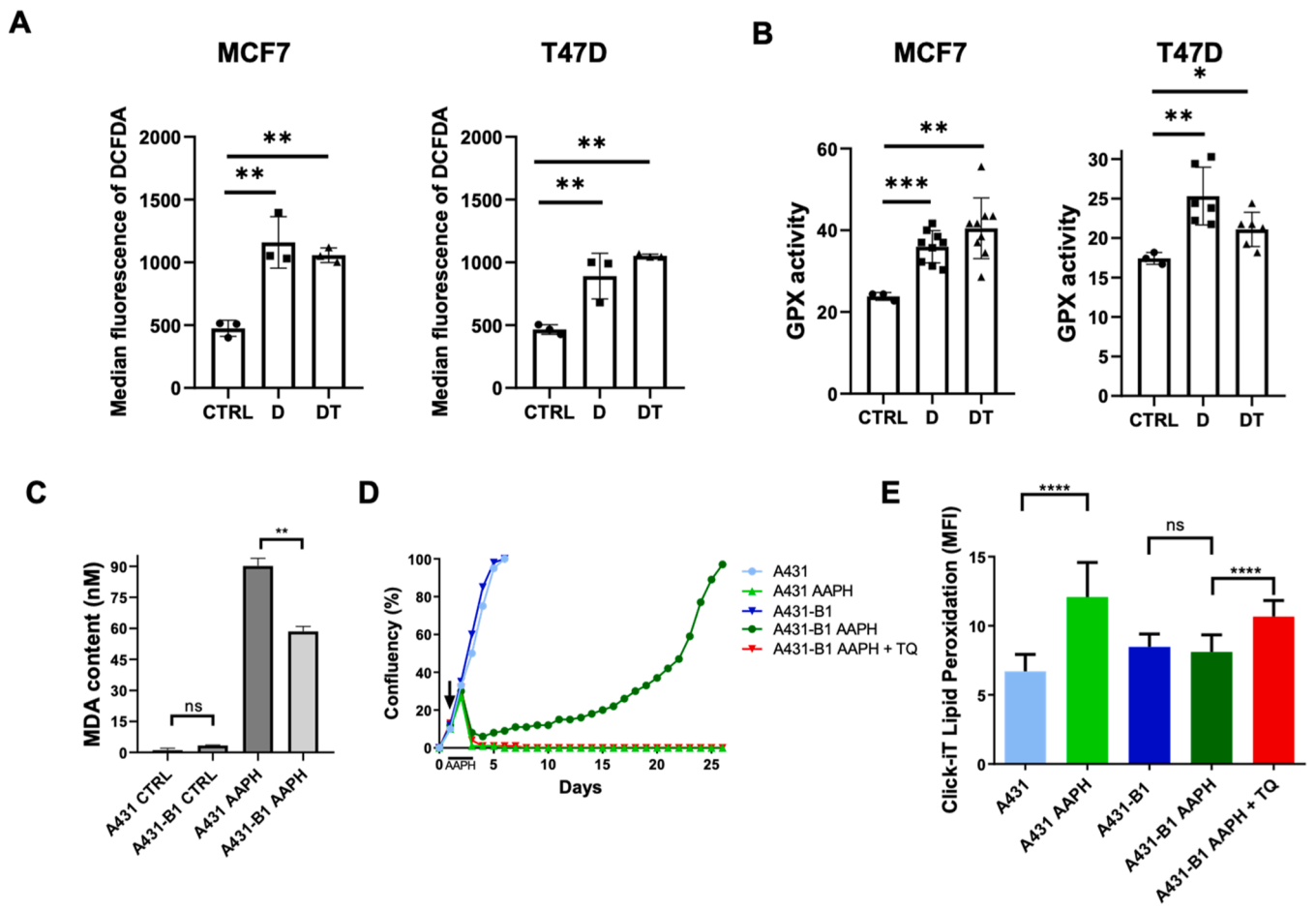

Fig. 5. Expression of P-gp contributes to long-term survival by clearing the cells of toxic lipid peroxidation products (A) ROS accumulation in MCF7 and T47D cells after 5 days of DOX treatment in the presence (DT) or absence (D) of Tariquidar. Control (CTRL): DCFDA fluorescence of untreated cells. (B) Glutathione peroxidase (GPX) activity in MCF7 and T47D cells after 5 days of DOX treatment in the presence (DT) or absence (D) of Tariquidar. (C) Malondialdehyde (MDA) concentrations in parental and ABCB1-expressing A431 cells with or without 10 mM AAPH treatment. (D) Repopulation assay of untreated (blue) and AAPH treated cells with and without TQ. Cells were treated with 10 mM AAPH for 48 h (arrow). Following the removal of AAPH, A431 (light green) or A431-B1cells were allowed to recover in the absence (dark green) or presence (red) of TQ.) (E) Extent of lipid peroxidation measured with the Click-iT Lipid Peroxidation Imaging kit (Thermo) at 24 h after 10 mM AAPH treatment.

mammary tumor bearing mice were treated with different combinations of doxorubicin and Tariquidar (Fig. 6A, Supplementary Fig. 15). Whereas saline- or TQ-treated mice had to be sacrificed within 20 days of tumor engraftment, treatment with the maximum tolerated dose (MTD) of doxorubicin increased the median survival of mice to 73 days. Addition of TQ 30 min prior DOX treatment (TD) or repeated administrations of TQ during doxorubicin drug holidays (D-T-T) resulted in a similar and significant increase in the relapse-free survival (Fig. 6B), without any effect on the overall survival of mice (Fig. 6C). Strikingly, a combined administration scheme of TQ 30 min after DOX treatment and then continued during DOX drug holidays (DT-T-T) resulted in a further increase of therapeutic efficiency, significantly prolonging relapse-free and overall survival. Analysis of doxorubicin pharmacokinetics indicated that the administration of Tariquidar following chemotherapy does not result in increased doxorubicin accumulation in the heart and liver (Supplementary Fig. 16). Importantly, treatment-naïve tumor pieces do not express P-gp (Fig. 6D), showing that TQ does not improve the efficiency of treatment by inhibiting the efflux of DOX from preexisting MDR cells. Yet the effect was P-gp dependent, as tumors lacking the *Abcb1a* and *Abcb1b* genes did not benefit from the addition of TQ to DOX treatment (Fig. 6E).

Discussion

Commonly used in vitro models of resistance rely on sequential drug treatments with increasing drug concentrations. Typically, such models reveal aberrations of the drug target pathways that confer advantage under the selective pressure of chemotherapy (Venkatesan et al., 2017), considered to occur through genetic selection of rare pre-existing clones equipped to survive and quickly re-grow, or through a therapy-induced increase in mutation rates (Russo et al., 2019). Recent focus on studying resistance mechanisms has shifted from characterizing acquired resistance to the study of resistance evolution, intratumoral heterogeneity, clonal and phenotypical selection during therapy (Zhao et al., 2016). In a seminal paper, Sharma and colleagues found that a subpopulation of cancer cells can maintain viability under conditions where the majority of the cancer is rapidly killed by the therapy (Sharma et al., 2010). Persistence of drug tolerant cells is not linked to genetic heterogeneity or de novo mutations. Rather, escape from drug-induced cell death and the awakening of dormant DTPs are governed by non-genetic mechanisms and adaptive phenotypes.

Here our aim was to characterize and evaluate transient phenotypes during acute chemotherapy response and long-term survival of 3 breast cancer cell lines with variable receptor status. Following a 5-day treatment with lethal concentrations of chemotherapeutic agents that resulted in overwhelming DNA damage across the cells (Figs. 1B, 3D),

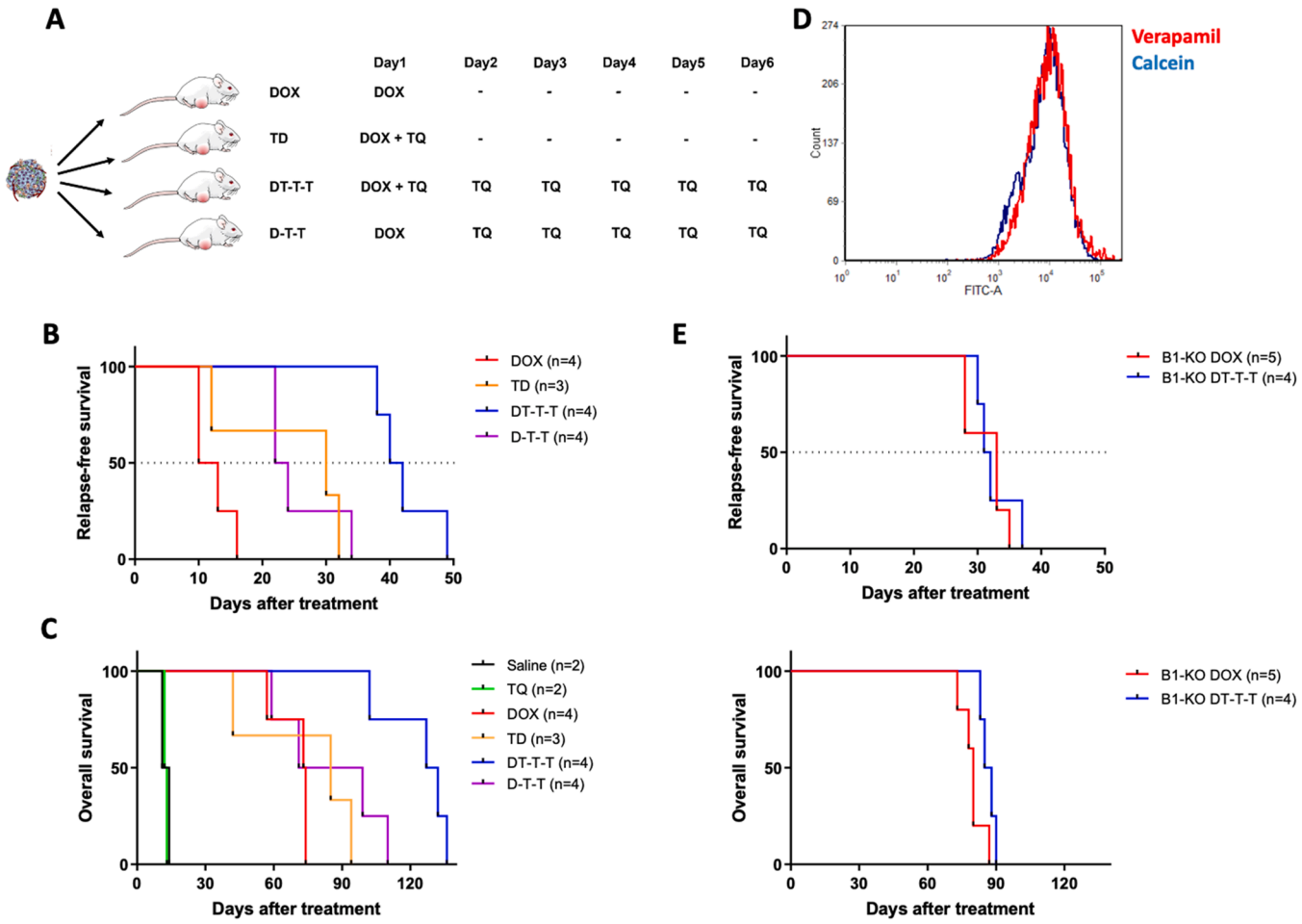

Fig. 6. Prolonged P-gp inhibition during doxorubicin treatment holidays increases relapse-free and overall survival in a clinically relevant mouse model of breast cancer. (A) Schematic representation of the different treatment strategies. At each treatment cycle, mice were treated with the maximum tolerated dose of doxorubicin without (DOX) or with (TD) the P-gp inhibitor TQ (TQ was administered 30 min prior to DOX). In the third group, TQ was administered 30 min after DOX and was maintained at each treatment cycle with daily injections for additional 5 days (DT-T-T). In the fourth group, DOX was administered as a monotherapy, followed at each treatment cycle with daily injections of TQ for 5 days (D-T-T). Treatment cycles were repeated when the tumors reached their initial volume. (B) Relapse-free survival of treatment groups. (C) Overall survival of treatment groups. (D) Drug-naive tumors lack Abcb1a revealed by the calcein assay. Verapamil (red) has no effect on the accumulation of calcein (blue), suggesting lack of efflux mediated by P-gp. (E) Relapse-free and overall survival of mice bearing Abcb1-KO tumors treated with either the DOX or DT-T-T protocol.

DTP cells appeared with characteristic hallmarks (Shen et al., 2020). DTP cells remained dormant for 3–4 weeks (Fig. 1F), showing wide-ranging phenotypic changes including EMT (Fig. 2). Consistent with previous observations of reversible drug tolerance, repopulating cells regained the phenotype and drug sensitivity of treatment-naïve cells (Fig. 3C). Similar results have been reported earlier, confirming the induced expression of P-gp in early drug resistance phenotype (Chaudhary and Roninson, 1993; Pisco et al., 2013). P-gp expression in MDR cells is attributed to the selection of pre-existing multi-drug-resistant cells, or the acquisition of complex genomic rearrangements of the MDR1 regulatory region (Mickley et al., 1997). In DTP cells, P-gp expression is induced by short term exposure to chemotherapeutic compounds, as part of the general cellular response triggered by cellular damage. A common trait of the applied chemotherapeutic agents is that they act as intracellular poisons, targeting dividing cells. However, transient upregulation of P-gp was detected only after treatment with doxorubicin and Olaparib, while cisplatin had no effect. The induction of detoxifying pathways is orchestrated by nuclear receptors and transcription factors that recognize xenobiotics and their metabolites as ligands (Chen et al., 2012). These regulatory processes converge to select for the most efficient set of proteins to protect the cells (Tóth et al., 2015). In that frame, lack of P-gp induction following cisplatin treatment can be explained by the fact that Olaparib (Lawlor et al., 2014) and doxorubicin are P-gp substrates, while cisplatin is not recognized by the ABCB1 pump (Szakács et al., 2004). Chemotherapy often produces cellular ROS, which in turn activates the collaboration of antioxidant factors with drug transporters (Liu et al., 2020; Mirzaei et al., 2022). The promoter of the ABCB1/P-glycoprotein gene contains several binding sites for transcription factors that respond to oxidative stress, hypoxia, xenobiotics and drugs (Scotto, 2003). It is also well established that EMT transcription factors and ERK phosphorylation can upregulate the expression of MDR transporters (Li et al., 2009; Saxena et al., 2011; Wang et al., 2014). In particular, the ERK-inhibitor U0126 was shown to fully reverse MDR by promoting the degradation of P-gp, without any effect on its biosynthesis (Katayama et al., 2007). By inhibiting the ERK pathway we efficiently prevented the doxorubicin-induced surge of P-gp expression, proving the link between ERK activation and P-gp expression in DTP cells (Fig. 2E).

Conventional wisdom would suggest that P-gp is upregulated to rid cells of drugs. Extended inhibition of P-gp in MDR cells beyond the removal of the drug from the culture medium was shown to significantly increase the effectiveness of the therapy (Nanayakkara et al., 2019). However, our results indicate that the benefit of P-gp expression in drug tolerant persister cells is not linked to drug efflux, as cells expressing

P-gp did not show decreased doxorubicin content (Fig. 4B), and the addition of TQ during or after DOX treatment did not change cellular fluorescence (Fig. 4C,D). Recent studies have revealed redox signaling as a major regulator of DTP cells (Oren et al., 2021; Zhang et al., 2023). Importantly, pharmacological inhibition of NRF2 or GPX4 was shown to prevent reactivation of dormant cells, indicating that the adaptive antioxidant response of DTP cells is a targetable trait (Fox et al., 2020; Wang et al., 2023). Based on reports suggesting that (i) P-gp can transport highly toxic oxidized lipids (Helvoort et al., 1996; Masuda et al., 2008); and (ii) the therapy resistant state is dependent on the lipid peroxidase pathway (Viswanathan et al., 2017), we hypothesized that P-gp promotes survival by clearing DTP cells of oxidatively fragmented membrane phospholipids. Indeed, P-gp expressing cells proved to be resistant to lipid peroxidation, and were sensitized to oxidizing agents by the P-gp inhibitor Tariquidar (Fig. 5). Although P-gp was also induced by a short-term treatment with Olaparib, addition of Tariquidar did not have any effect. Similarly, inhibition of P-gp in paclitaxel-induced persister cells did not translate into inhibition of secondary resistance to EGFR-TKIs (Aldonza et al., 2020). However, since PARP-inhibition is associated with the decrease, rather than the increase of ROS (Ahmad et al., 2019; Jagtap and Szabó, 2005) (Supplementary Fig. 10), inhibition of P-gp function is not expected to have any influence on the survival of Olaparib-induced DTP cells.

Inhibiting drug efflux has been long hypothesized as a means to improve treatment outcome of multidrug resistant cancer. Unfortunately, clinical trials conducted with third-generation inhibitors such as Tariquidar have failed to demonstrate benefit (Cripe et al., 2010). The disappointing results led to the discontinuation of the development of inhibitors, even though recent studies have provided further evidence in support of the relevance of ABC transporters in the clinical drug resistance of at least a subset of cancers (Robey et al., 2018). In the trials, inhibitors were typically administered an hour before the start of chemotherapy to reach maximum inhibitory effect preventing the cellular efflux of the anticancer drugs (Cripe et al., 2010; Fox et al., 2015). Unfortunately, this protocol significantly increased the toxic side effect of the concomitantly administered chemotherapy due to the inhibition of P-gp activity in pharmacological barriers such as the blood-brain-barrier. The *K14cre;Brca1*$^{F/F}$*;p53*$^{F/F}$ mouse model of hereditary breast cancer has been successfully used to study mechanisms of acquired resistance (Rottenberg and Borst, 2012). Orthotopically transplanted Brca/p53-deficient tumors develop mammary adenocarcinomas that retain histomorphological features, molecular characteristics and the drug sensitivity profile of the original model (Rottenberg et al., 2007). As treatment-naïve tumors do not express P-glycoprotein (Fig. 6D), they initially respond to treatment with the maximal tolerated dose of doxorubicin. However, after multiple treatment cycles, the tumors always acquire resistance based on the increased expression of Abcb1 (Rottenberg et al., 2007). In the same model, administration of Tariquidar 30 min prior to chemotherapy was shown to resensitize multidrug resistant tumors, while Tariquidar alone had no effect on tumor growth (Rottenberg et al., 2008). Our in vitro experiments indicating that inhibition of P-gp function following the removal of doxorubicin can prevent the long-term survival of DTP cells (Fig. 4), prompted us to test a new therapeutic protocol, in which Tariquidar is administered prior to the onset of MDR. Our earlier results indicated the rapid decay of doxorubicin plasma levels (doxorubicin levels cannot be detected 3 h after intravenous injection (Füredi et al., 2017a; Kannan et al., 2020), which allowed us to administer Tariquidar without the risk of potentially toxic pharmacodynamic interactions with doxorubicin (Supplementary Fig. 16). Administration of Tariquidar during doxorubicin treatment holidays resulted in a significant increase in the overall survival of mice (Fig. 6). To test whether the effect of Tariquidar is indeed linked to the inhibition of P-gp function, we repeated the experiments with P-gp deficient tumors. P-gp–deficient mice carrying spontaneous mammary tumors cannot be treated with the MTD of doxorubicin because P-gp contributes to the protection of pharmacological sanctuaries (Schinkel et al., 1994). However, the tumoral role of P-gp can be studied by engrafting wild-type mice with *Brca1*$^{-/-}$*;p53*$^{-/-}$*;Abcb1a/b*$^{-/-}$ tumors, as lack of P-gp does not affect the latency or morphology of the tumors. Similarly to published results (Rottenberg et al., 2012), P-gp deficient tumors were hypersensitive to doxorubicin treatment, even if tumors eventually acquired resistance. Significantly, administration of Tariquidar did not have any effect, providing strong evidence that the prolonged survival of P-gp proficient tumors treated by the preemptive Tariquidar protocol is due to the inhibition of P-glycoprotein function.

Taken together, these results demonstrate that P-gp inhibitors can have a beneficial effect before the onset of doxorubicin resistance, via a mechanism unrelated to the inhibition of drug efflux. While P-gp inhibitors such as Tariquidar or Zosuquidar did not provide clinical benefit due to enhanced toxicity of coadministered anticancer drug(s), third-generation inhibitors devoid of intrinsic pharmacological activity have successfully passed early-phase trials, providing ample evidence of their clinical safety. Although a multitude of potential therapeutic approaches to target cancer persistence have been postulated, as yet none has been successfully translated into clinical use (Shen et al., 2020; Fong et al. 2021). The Brca/p53-deficient mammary tumor model recapitulates several key features of human BRCA1-associated breast cancer, and is therefore considered to be a good predictor for clinical responses of BRCA1-deficient cancers (Liu et al., 2007). Based on the results presented in this manuscript we suggest that a new therapeutic regimen, comprising of the prolonged administration of a P-gp inhibitor during drug holidays would likely benefit patients without the risk of aggravated side effects related to the concomitantly administered toxic chemotherapy. Understanding which tumor subtypes have a propensity for cell-state plasticity, whether specific therapeutics trigger DTP transitions, and what targetable epigenomic processes underlie these transitions will be critical steps to improving management of heterogeneous breast tumors (Risom et al., 2018; Musyuni et al., 2022). Effective targeting of DTPs will result in a paradigm shift, changing the focus from countering drug resistance mechanisms to preventing or delaying therapy resistance, leading to improved treatments of patients.

CRediT authorship contribution statement

Conceptualization: Kornélia Szebényi, András Füredi, Gergely Szakács. Methodology: Kornélia Szebényi, András Füredi, Eszter Bajtai, Sai Nagender Sama, Ágnes Csiszár, Balázs Gombos, Michael Grusch, Pál Szabó. Formal analysis and investigation: Kornélia Szebényi, András Füredi, Gergely Szakács. Writing: Kornélia Szebényi, András Füredi, Gergely Szakács. Supervision: Gergely Szakács. All authors read and approved the final manuscript.

Declaration of Competing Interest

The authors declare that they have no known competing financial interests or personal relationships that could have appeared to influence the work reported in this paper.

Acknowledgments

This work was supported by REAP (H2020-ICT-2020-2, Grant Agreement ID 101016964) to GS and AC, RRF-2.3.1-21-2022-00015 and 2019-1.3.1-KK-2019-00007 (Hungarian National Research, Development and Innovation Office) to GS and AF, City of Vienna Fund for Innovative Interdisciplinary Cancer Research (21132) to MG, HORIZON-WIDERA-2022-TALENTS-02-01-101090302) and VEKOP-2.3.3-15-2017-00014 to KS and HORIZON.1.2 - Marie Skłodowska-Curie Actions (MSCA) Postdoctoral Fellowship (POC-TDM Grant agreement ID: 101065044) to AF.

Appendix A. Supporting information

Supplementary data associated with this article can be found in the online version at doi:10.1016/j.drup.2023.101007.

References

Ahmad, A., Vieira, J., de, C., de Mello, A.H., de Lima, T.M., Ariga, S.K., Barbeiro, D.F., Barbeiro, H.V., Szczesny, B., Törö, G., Druzhyna, N., Randi, E.B., Marcatti, M., Toliver-Kinsky, T., Kiss, A., Liaudet, L., Salomao, R., Soriano, F.G., Szabo, C., 2019. The PARP inhibitor olaparib exerts beneficial effects in mice subjected to cecal ligature and puncture and in cells subjected to oxidative stress without impairing DNA integrity: a potential opportunity for repurposing a clinically used oncological drug for the experimental therapy of sepsis. Pharmacol. Res. 145, 104263 https://doi.org/10.1016/j.phrs.2019.104263.

Aissa, A.F., Islam, A.B.M.M.K., Ariss, M.M., Go, C.C., Rader, A.E., Conrardy, R.D., Gajda, A.M., Rubio-Perez, C., Valyi-Nagy, K., Pasquinelli, M., Feldman, L.E., Green, S.J., Lopez-Bigas, N., Frolov, M.V., Benevolenskaya, E.V., 2021. Single-cell transcriptional changes associated with drug tolerance and response to combination therapies in cancer. Nat. Commun. 12 (1), 1628 https://doi.org/10.1038/s41467-021-21884-z.

Aldonza, M.B.D., Ku, J., Hong, J.-Y., Kim, D., Yu, S.J., Lee, M.-S., Prayogo, M.C., Tan, S., Kim, D., Han, J., Lee, S.K., Im, S.G., Ryu, H.S., Kim, Y., 2020. Prior acquired resistance to paclitaxel relays diverse EGFR-targeted therapy persistence mechanisms. Sci. Adv. 6 (6), eaav7416 https://doi.org/10.1126/sciadv.aav7416.

Borst, P., 2012. Cancer drug pan-resistance: pumps, cancer stem cells, quiescence, epithelial to mesenchymal transition, blocked cell death pathways, persisters or what? Open Biol. 2 (5) https://doi.org/10.1098/rsob.120066.

Chaudhary, P.M., Roninson, I.B., 1993. Induction of multidrug resistance in human cells by transient exposure to different chemotherapeutic drugs. JNCI J. Natl. Cancer Inst. 85 (8), 632–639. https://doi.org/10.1093/jnci/85.8.632.

Chen, Y., Tang, Y., Guo, C., Wang, J., Boral, D., Nie, D., 2012. Nuclear receptors in the multidrug resistance through the regulation of drug-metabolizing enzymes and drug transporters. Biochem. Pharmacol. 83 (8), 1112–1126. https://doi.org/10.1016/j.bcp.2012.01.030.

Cripe, L.D., Uno, H., Paietta, E.M., Litzow, M.R., Ketterling, R.P., Bennett, J.M., Rowe, J. M., Lazarus, H.M., Luger, S., Tallman, M.S., 2010. Zosuquidar, a novel modulator of P-glycoprotein, does not improve the outcome of older patients with newly diagnosed acute myeloid leukemia: a randomized, placebo-controlled trial of the Eastern Cooperative Oncology Group 3999. Blood 116 (20), 4077–4085. https://doi.org/10.1182/blood-2010-04-277269.

Cserepes, M., Türk, D., Tóth, S., Pape, V.F.S., Gaál, A., Gera, M., Szabó, J.E., Kucsma, N., Várady, G., Vértessy, B.G., Streli, C., Szabó, P.T., Tovari, J., Szoboszlai, N., Szakács, G., 2020. Unshielding multidrug resistant cancer through selective iron depletion of P-glycoprotein–expressing cells. Cancer Res. 80 (4), 663–674. https://doi.org/10.1158/0008-5472.CAN-19-1407.

Duarte, A.A., Gogola, E., Sachs, N., Barazas, M., Annunziato, S., R de Ruiter, J., Velds, A., Blatter, S., Houthuijzen, J.M., van de Ven, M., Clevers, H., Borst, P., Jonkers, J., Rottenberg, S., 2018. BRCA-deficient mouse mammary tumor organoids to study cancer-drug resistance. Nat. Methods 15 (2), 134–140. https://doi.org/10.1038/nmeth.4535.

Echeverria, G.V., Ge, Z., Seth, S., Zhang, X., Jeter-Jones, S., Zhou, X., Cai, S., Tu, Y., McCoy, A., Peoples, M., Sun, Y., Qiu, H., Chang, Q., Bristow, C., Carugo, A., Shao, J., Ma, X., Harris, A., Mundi, P., Lau, R., Ramamoorthy, V., Wu, Y., Alvarez, M.J., Califano, A., Moulder, S.L., Symmans, W.F., Marszalek, J.R., Heffernan, T.P., Chang, J.T., Piwnica-Worms, H., 2019. Resistance to neoadjuvant chemotherapy in triple-negative breast cancer mediated by a reversible drug-tolerant state. Sci. Transl. Med. 11 (488) https://doi.org/10.1126/scitranslmed.aav0936.

Fong, D., Christensen, C.T., Chan, M.M., 2021. Targeting cancer stem cells with repurposed drugs to improve current therapies. Recent Patents Anticancer Drug Discov. 16 (2), 136–160.

Fox, D.B., Garcia, N.M.G., McKinney, B.J., Lupo, R., Noteware, L.C., Newcomb, R., Liu, J., Locasale, J.W., Hirschey, M.D., Alvarez, J.V., 2020. NRF2 activation promotes the recurrence of dormant tumour cells through regulation of redox and nucleotide metabolism. Nat. Metab. 2 (4), 318–334. https://doi.org/10.1038/s42255-020-0191-z.

Fox, E., Widemann, B.C., Pastakia, D., Chen, C.C., Yang, S.X., Cole, D., Balis, F.M., 2015. Pharmacokinetic and pharmacodynamic study of tariquidar (XR9576), a P-glycoprotein inhibitor, in combination with doxorubicin, vinorelbine, or docetaxel in children and adolescents with refractory solid tumors. Cancer Chemother. Pharmacol. 76 (6), 1273–1283. https://doi.org/10.1007/s00280-015-2845-1.

Füredi, A., Szebényi, K., Tóth, S., Cserepes, M., Hámori, L., Nagy, V., Karai, E., Vajdovich, P., Imre, T., Szabó, P., Szüts, D., Tóvári, J., Szakács, G., 2017a. Pegylated liposomal formulation of doxorubicin overcomes drug resistance in a genetically engineered mouse model of breast cancer. J. Control. Release 261, 287–296. https://doi.org/10.1016/j.jconrel.2017.07.010.

Füredi, A., Tóth, S., Szebényi, K., Pape, V.F.S., Türk, D., Kucsma, N., Cervenak, L., Tóvári, J., Szakács, G., 2017b. Identification and validation of compounds selectively killing resistant cancer: delineating cell line–specific effects from P-glycoprotein–induced toxicity. Mol. Cancer Ther. 16 (1), 45–56. https://doi.org/10.1158/1535-7163.MCT-16-0333-T.

Hámori, L., Kudlik, G., Szebényi, K., Kucsma, N., Szeder, B., Póti, Á., Uher, F., Várady, G., Szüts, D., Tóvári, J., Füredi, A., Szakács, G., 2020. Establishment and characterization of a Brca1−/−, P53−/− mouse mammary tumor cell line. Int. J. Mol. Sci. 21 (4), 1185. https://doi.org/10.3390/ijms21041185.

Hangauer, M.J., Viswanathan, V.S., Ryan, M.J., Bole, D., Eaton, J.K., Matov, A., Galeas, J., Dhruv, H.D., Berens, M.E., Schreiber, S.L., McCormick, F., McManus, M. T., 2017. Drug-tolerant persister cancer cells are vulnerable to GPX4 inhibition. Nature 551 (7679), 247–250. https://doi.org/10.1038/nature24297.

Harbeck, N., Penault-Llorca, F., Cortes, J., Gnant, M., Houssami, N., Poortmans, P., Ruddy, K., Tsang, J., Cardoso, F., 2019. Breast cancer. Nat. Rev. Dis. Prim. 5 (1), 1–31. https://doi.org/10.1038/s41572-019-0111-2.

Isakoff, S.J., 2010. Triple negative breast cancer: role of specific chemotherapy agents. Cancer J. Sudbury Mass 16 (1), 53–61. https://doi.org/10.1097/PPO.0b013e3181d24ff7.

Jagtap, P., Szabó, C., 2005. Poly(ADP-Ribose) polymerase and the therapeutic effects of its inhibitors. Nat. Rev. Drug Discov. 4 (5), 421–440. https://doi.org/10.1038/nrd1718.

Kannan, P., Füredi, A., Dizdarevic, S., Wanek, T., Mairinger, S., Collins, J., Falls, T., van Dam, R.M., Maheshwari, D., Lee, J.T., Szakács, G., Langer, O., 2020. In vivo characterization of [18F]AVT-011 as a radiotracer for PET imaging of multidrug resistance. Eur. J. Nucl. Med. Mol. Imaging 47 (8), 2026–2035. https://doi.org/10.1007/s00259-019-04589-w.

Katayama, K., Yoshioka, S., Tsukahara, S., Mitsuhashi, J., Sugimoto, Y., 2007. Inhibition of the mitogen-activated protein kinase pathway results in the down-regulation of P-glycoprotein. Mol. Cancer Ther. 6 (7), 2092–2102. https://doi.org/10.1158/1535-7163.MCT-07-0148.

Lawlor, D., Martin, P., Busschots, S., Thery, J., O'Leary, J.J., Hennessy, B.T., Stordal, B., 2014. PARP Inhibitors as P-glyoprotein substrates. J. Pharm. Sci. 103 (6), 1913–1920. https://doi.org/10.1002/jps.23952.

Li, Q.-Q., Xu, J.-D., Wang, W.-J., Cao, X.-X., Chen, Q., Tang, F., Chen, Z.-Q., Liu, X.-P., Xu, Z.-D., 2009. Twist1-mediated adriamycin-induced epithelial-mesenchymal transition relates to multidrug resistance and invasive potential in breast cancer cells. Clin. Cancer Res. J. Am. Assoc. Cancer Res. 15 (8), 2657–2665. https://doi.org/10.1158/1078-0432.CCR-08-2372.

Liau, B.B., Sievers, C., Donohue, L.K., Gillespie, S.M., Flavahan, W.A., Miller, T.E., Venteicher, A.S., Hebert, C.H., Carey, C.D., Rodig, S.J., Shareef, S.J., Najm, F.J., van Galen, P., Wakimoto, H., Cahill, D.P., Rich, J.N., Aster, J.C., Suvà, M.L., Patel, A.P., Bernstein, B.E., 2017. Adaptive chromatin remodeling drives glioblastoma stem cell plasticity and drug tolerance. Cell Stem Cell 20 (2), 233–246.e7. https://doi.org/10.1016/j.stem.2016.11.003.

Liedtke, C., Mazouni, C., Hess, K.R., André, F., Tordai, A., Mejia, J.A., Symmans, W.F., Gonzalez-Angulo, A.M., Hennessy, B., Green, M., Cristofanilli, M., Hortobagyi, G.N., Pusztai, L., 2008. Response to neoadjuvant therapy and long-term survival in patients with triple-negative breast cancer. J. Clin. Oncol. 26 (8), 1275–1281. https://doi.org/10.1200/JCO.2007.14.4147.

Liu, J., Zhu, M., Feng, Y., Tang, Q., Xu, M., 2020. The multidrug resistance can be reversed for the decrease of P-Gp and LRP by inhibiting PI3K/Akt/NF-KB signal pathway in nasopharynx carcinoma. BSR20190239 Biosci. Rep. 40 (5). https://doi.org/10.1042/BSR20190239.

Liu, X., Holstege, H., van der Gulden, H., Treur-Mulder, M., Zevenhoven, J., Velds, A., Kerkhoven, R.M., van Vliet, M.H., Wessels, L.F.A., Peterse, J.L., Berns, A., Jonkers, J., 2007. Somatic loss of BRCA1 and P53 in mice induces mammary tumors with features of human BRCA1-mutated basal-like breast cancer. Proc. Natl. Acad. Sci. 104 (29), 12111–12116. https://doi.org/10.1073/pnas.0702969104.

Markowitz, D., Goff, S., Bank, A., 1988. A safe packaging line for gene transfer: separating viral genes on two different plasmids. J. Virol. 62 (4), 1120–1124. https://doi.org/10.1128/JVI.62.4.1120-1124.1988.

Masuda, M., Nakai, E., Mizutani, T., 2008. Study of oxidized lipids as endogenous substrates of P-Gp (ABCB1). Drug Metab. Lett. 2 (4), 238–244. https://doi.org/10.2174/187231208786734139.

Mickley, L.A., Spengler, B.A., Knutsen, T.A., Biedler, J.L., Fojo, T., 1997. Gene rearrangement: a novel mechanism for MDR-1 gene activation. J. Clin. Invest. 99 (8), 1947–1957. https://doi.org/10.1172/JCI119362.

Mirzaei, S., Gholami, M.H., Hashemi, F., Zabolian, A., Farahani, M.V., Hushmandi, K., Zarrabi, A., Goldman, A., Ashrafizadeh, M., Orive, G., 2022. Advances in understanding the role of P-Gp in doxorubicin resistance: molecular pathways, therapeutic strategies, and prospects. Drug Discov. Today 27 (2), 436–455. https://doi.org/10.1016/j.drudis.2021.09.020.

Musyuni, P., Bai, J., Sheikh, A., Vasanthan, K.S., Jain, G.K., Abourehab, M.A.S., Lather, V., Aggarwal, G., Kesharwani, P., Pandita, D., 2022. Precision medicine: ray of hope in overcoming cancer multidrug resistance. Drug Resist. Update 65, 100889. https://doi.org/10.1016/j.drup.2022.100889.

Myers, C.E., McGuire, W.P., Liss, R.H., Ifrim, I., Grotzinger, K., Young, R.C., 1977. Adriamycin: the role of lipid peroxidation in cardiac toxicity and tumor response. Science 197 (4299), 165–167. https://doi.org/10.1126/science.877547.

Nabil Benchekroun, M., Robert, J., 1992. Measurement of doxorubicin-induced lipid peroxidation under the conditions that determine cytotoxicity in cultured tumor cells. Anal. Biochem. 201 (2), 326–330. https://doi.org/10.1016/0003-2697(92)90346-9.

Nanayakkara, A.K., Vogel, P.D., Wise, J.G., 2019. Prolonged inhibition of P-glycoprotein after exposure to chemotherapeutics increases cell mortality in multidrug resistant cultured cancer cells. PLOS ONE 14 (6), e0217940. https://doi.org/10.1371/journal.pone.0217940.

Oren, Y., Tsabar, M., Cuoco, M.S., Amir-Zilberstein, L., Cabanos, H.F., Hütter, J.-C., Hu, B., Thakore, P.I., Tabaka, M., Fulco, C.P., Colgan, W., Cuevas, B.M., Hurvitz, S. A., Slamon, D.J., Deik, A., Pierce, K.A., Clish, C., Hata, A.N., Zaganjor, E., Lahav, G., Politi, K., Brugge, J.S., Regev, A., 2021. Cycling cancer persister cells arise from

lineages with distinct programs. Nature 596 (7873), 576–582. https://doi.org/10.1038/s41586-021-03796-6.
Pape, V.F.S., Türk, D., Szabó, P., Wiese, M., Enyedy, E.A., Szakács, G., 2015. Synthesis and characterization of the anticancer and metal binding properties of novel pyrimidinylhydrazone derivatives. J. Inorg. Biochem. 144, 18–30. https://doi.org/10.1016/j.jinorgbio.2014.12.015.
Pape, V.F.S., Gaál, A., Szatmári, I., Kucsma, N., Szoboszlai, N., Streli, C., Fülöp, F., Enyedy, É.A., Szakács, G., 2021. Relation of metal-binding property and selective toxicity of 8-hydroxyquinoline derived mannich bases targeting multidrug resistant cancer cells. Cancers 13 (1), 154. https://doi.org/10.3390/cancers13010154.
Pisco, A.O., Brock, A., Zhou, J., Moor, A., Mojtahedi, M., Jackson, D., Huang, S., 2013. Non-Darwinian dynamics in therapy-induced cancer drug resistance. Nat. Commun. 4 (1), 2467 https://doi.org/10.1038/ncomms3467.
Ramirez, M., Rajaram, S., Steininger, R.J., Osipchuk, D., Roth, M.A., Morinishi, L.S., Evans, L., Ji, W., Hsu, C.-H., Thurley, K., Wei, S., Zhou, A., Koduru, P.R., Posner, B. A., Wu, L.F., Altschuler, S.J., 2016. Diverse drug-resistance mechanisms can emerge from drug-tolerant cancer persister cells. Nat. Commun. 7 (1), 10690 https://doi.org/10.1038/ncomms10690.
Rehman, S.K., Haynes, J., Collignon, E., Brown, K.R., Wang, Y., Nixon, A.M.L., Bruce, J. P., Wintersinger, J.A., Mer, A.S., Lo, E.B.L., Leung, C., Lima-Fernandes, E., Pedley, N. M., Soares, F., McGibbon, S., He, H.H., Pollet, A., Pugh, T.J., Haibe-Kains, B., Morris, Q., Ramalho-Santos, M., Goyal, S., Moffat, J., O'Brien, C.A., 2021. Colorectal cancer cells enter a diapause-like DTP state to survive chemotherapy. Cell 184 (1), 226–242.e21. https://doi.org/10.1016/j.cell.2020.11.018.
Risom, T., Langer, E.M., Chapman, M.P., Rantala, J., Fields, A.J., Boniface, C., Alvarez, M.J., Kendsersky, N.D., Pelz, C.R., Johnson-Camacho, K., Dobrolecki, L.E., Chin, K., Aswani, A.J., Wang, N.J., Califano, A., Lewis, M.T., Tomlin, C.J., Spellman, P.T., Adey, A., Gray, J.W., Sears, R.C., 2018. Differentiation-state plasticity is a targetable resistance mechanism in basal-like breast cancer. Nat. Commun. 9 (1), 3815 https://doi.org/10.1038/s41467-018-05729-w.
Robey, R.W., Pluchino, K.M., Hall, M.D., Fojo, A.T., Bates, S.E., Gottesman, M.M., 2018. Revisiting the role of ABC transporters in multidrug-resistant cancer. Nat. Rev. Cancer 18 (7), 452–464. https://doi.org/10.1038/s41568-018-0005-8.
Roesch, A., Vultur, A., Bogeski, I., Wang, H., Zimmermann, K.M., Speicher, D., Körbel, C., Laschke, M.W., Gimotty, P.A., Philipp, S.E., Krause, E., Pätzold, S., Villanueva, J., Krepler, C., Fukunaga-Kalabis, M., Hoth, M., Bastian, B.C., Vogt, T., Herlyn, M., 2013. Overcoming intrinsic multidrug resistance in melanoma by blocking the mitochondrial respiratory chain of slow-cycling JARID1Bhigh cells. Cancer Cell 23 (6), 811–825. https://doi.org/10.1016/j.ccr.2013.05.003.
Rottenberg, S., Borst, P., 2012. Drug resistance in the mouse cancer clinic. Drug Resist. Update 15 (1), 81–89. https://doi.org/10.1016/j.drup.2012.01.001.
Rottenberg, S., Nygren, A.O.H., Pajic, M., van Leeuwen, F.W.B., van der Heijden, I., van de Wetering, K., Liu, X., de Visser, K.E., Gilhuijs, K.G., van Tellingen, O., Schouten, J. P., Jonkers, J., Borst, P., 2007. Selective induction of chemotherapy resistance of mammary tumors in a conditional mouse model for hereditary breast cancer. Proc. Natl. Acad. Sci. 104 (29), 12117–12122. https://doi.org/10.1073/pnas.0702955104.
Rottenberg, S., Jaspers, J.E., Kersbergen, A., van der Burg, E., Nygren, A.O.H., Zander, S. A.L., Derksen, P.W.B., de Bruin, M., Zevenhoven, J., Lau, A., Boulter, R., Cranston, A., O'Connor, M.J., Martin, N.M.B., Borst, P., Jonkers, J., 2008. High sensitivity of BRCA1-deficient mammary tumors to the PARP inhibitor AZD2281 alone and in combination with platinum drugs. Proc. Natl. Acad. Sci. 105 (44), 17079–17084. https://doi.org/10.1073/pnas.0806092105.
Rottenberg, S., Vollebergh, M.A., de Hoon, B., de Ronde, J., Schouten, P.C., Kersbergen, A., Zander, S.A.L., Pajic, M., Jaspers, J.E., Jonkers, M., Lodén, M., Sol, W., van der Burg, E., Wesseling, J., Gillet, J.-P., Gottesman, M.M., Gribnau, J., Wessels, L., Linn, S.C., Jonkers, J., Borst, P., 2012. Impact of intertumoral heterogeneity on predicting chemotherapy response of BRCA1-deficient mammary tumors. Cancer Res. 72 (9), 2350–2361. https://doi.org/10.1158/0008-5472.CAN-11-4201.
Russo, M., Crisafulli, G., Sogari, A., Reilly, N.M., Arena, S., Lamba, S., Bartolini, A., Amodio, V., Magrì, A., Novara, L., Sarotto, I., Nagel, Z.D., Piett, C.G., Amatu, A., Sartore-Bianchi, A., Siena, S., Bertotti, A., Trusolino, L., Corigliano, M., Gherardi, M., Lagomarsino, M.C., Di Nicolantonio, F., Bardelli, A., 2019. Adaptive mutability of colorectal cancers in response to targeted therapies. eaav4474 Science. https://doi.org/10.1126/science.aav4474.
Saxena, M., Stephens, M.A., Pathak, H., Rangarajan, A., 2011. Transcription factors that mediate epithelial–mesenchymal transition lead to multidrug resistance by upregulating ABC transporters. e179–e179 Cell Death Dis. 2 (7). https://doi.org/10.1038/cddis.2011.61.
Schinkel, A.H., Smit, J.J.M., van Tellingen, O., Beijnen, J.H., Wagenaar, E., van Deemter, L., Mol, C.A.A.M., van der Valk, M.A., Robanus-Maandag, E.C., te Riele, H. P.J., Berns, A.J.M., Borst, P., 1994. Disruption of the mouse Mdr1a P-glycoprotein gene leads to a deficiency in the blood-brain barrier and to increased sensitivity to drugs. Cell 77 (4), 491–502. https://doi.org/10.1016/0092-8674(94)90212-7.
Scotto, K.W., 2003. Transcriptional regulation of ABC drug transporters. Oncogene 22 (47), 7496–7511. https://doi.org/10.1038/sj.onc.1206950.
Sharma, S.V., Lee, D.Y., Li, B., Quinlan, M.P., Takahashi, F., Maheswaran, S., McDermott, U., Azizian, N., Zou, L., Fischbach, M.A., Wong, K.-K., Brandstetter, K., Wittner, B., Ramaswamy, S., Classon, M., Settleman, J., 2010. A chromatin-mediated reversible drug-tolerant state in cancer cell subpopulations. Cell 141 (1), 69–80. https://doi.org/10.1016/j.cell.2010.02.027.
Shen, S., Vagner, S., Robert, C., 2020. Persistent cancer cells: the deadly survivors. Cell 183 (4), 860–874. https://doi.org/10.1016/j.cell.2020.10.027.
Shukla, A., Hillegass, J.M., MacPherson, M.B., Beuschel, S.L., Vacek, P.M., Pass, H.I., Carbone, M., Testa, J.R., Mossman, B.T., 2010. Blocking of ERK1 and ERK2 sensitizes human mesothelioma cells to doxorubicin. Mol. Cancer 9, 314. https://doi.org/10.1186/1476-4598-9-314.
Szakács, G., Annereau, J.-P., Lababidi, S., Shankavaram, U., Arciello, A., Bussey, K.J., Reinhold, W., Guo, Y., Kruh, G.D., Reimers, M., Weinstein, J.N., Gottesman, M.M., 2004. Predicting drug sensitivity and resistance: profiling ABC transporter genes in cancer cells. Cancer Cell 6 (2), 129–137. https://doi.org/10.1016/j.ccr.2004.06.026.
Szakács, G., Paterson, J.K., Ludwig, J.A., Booth-Genthe, C., Gottesman, M.M., 2006. Targeting multidrug resistance in cancer. Nat. Rev. Drug Discov. 5 (3), 219–234.
Tóth, A., Brózik, A., Szakács, G., Sarkadi, B., Hegedüs, T., 2015. A novel mathematical model describing adaptive cellular drug metabolism and toxicity in the chemoimmune system. PLOS ONE 10 (2), e0115533. https://doi.org/10.1371/journal.pone.0115533.
van Helvoort, A., Smith, A.J., Sprong, H., Fritzsche, I., Schinkel, A.H., Borst, P., Meer, G. van, 1996. MDR1 P-glycoprotein is a lipid translocase of broad specificity, while MDR3 P-glycoprotein specifically translocates phosphatidylcholine. Cell 87 (3), 507–517. https://doi.org/10.1016/S0092-8674(00)81370-7.
Venkatesan, S., Swanton, C., Taylor, B.S., Costello, J.F., 2017. Treatment-induced mutagenesis and selective pressures sculpt cancer evolution. Cold Spring Harb. Perspect. Med. 7 (8) https://doi.org/10.1101/cshperspect.a026617.
Viswanathan, V.S., Ryan, M.J., Dhruv, H.D., Gill, S., Eichhoff, O.M., Seashore-Ludlow, B., Kaffenberger, S.D., Eaton, J.K., Shimada, K., Aguirre, A.J., Viswanathan, S.R., Chattopadhyay, S., Tamayo, P., Yang, W.S., Rees, M.G., Chen, S., Boskovic, Z.V., Javaid, S., Huang, C., Wu, X., Tseng, Y.-Y., Roider, E.M., Gao, D., Cleary, J.M., Wolpin, B.M., Mesirov, J.P., Haber, D.A., Engelman, J.A., Boehm, J.S., Kotz, J.D., Hon, C.S., Chen, Y., Hahn, W.C., Levesque, M.P., Doench, J.G., Berens, M.E., Shamji, A.F., Clemons, P.A., Stockwell, B.R., Schreiber, S.L., 2017. Dependency of a therapy-resistant state of cancer cells on a lipid peroxidase pathway. Nature 547 (7664), 453–457. https://doi.org/10.1038/nature23007.
Wang, Y., Ma, G., Wang, Q., Wen, M., Xu, Y., He, X., Zhang, P., Wang, Y., Yang, T., Zhan, P., Wei, G., 2014. Involvement of CUL4A in regulation of multidrug resistance to P-Gp substrate drugs in breast cancer cells. Molecules 19 (1), 159–176. https://doi.org/10.3390/molecules19010159.
Wang, Y., Wu, X., Ren, Z., Li, Y., Zou, W., Chen, J., Wang, H., 2023. Overcoming cancer chemotherapy resistance by the induction of ferroptosis. Drug Resist. Update 66, 100916. https://doi.org/10.1016/j.drup.2022.100916.
Zhang, Z., Tan, Y., Huang, C., Wei, X., 2023. Redox signaling in drug-tolerant persister cells as an emerging therapeutic target. eBioMedicine 89. https://doi.org/10.1016/j.ebiom.2023.104483.
Zhao, B., Sedlak, J.C., Srinivas, R., Creixell, P., Pritchard, J.R., Tidor, B., Lauffenburger, D.A., Hemann, M.T., 2016. Exploiting temporal collateral sensitivity in tumor clonal evolution. Cell 165 (1), 234–246. https://doi.org/10.1016/j.cell.2016.01.045.
Zhao, J., Zhang, H., Lei, T., Liu, J., Zhang, S., Wu, N., Sun, B., Wang, M., 2020. Drug resistance gene expression and chemotherapy sensitivity detection in Chinese women with different molecular subtypes of breast cancer. Cancer Biol. Med. 17 (4), 1014–1025. https://doi.org/10.20892/j.issn.2095-3941.2020.0157.